Molecular Human Reproduction, Vol.26, No.4, pp. 256–268, 2020
Advance Access Publication on February 5, 2020 doi:10.1093/molehr/gaaa013

molecular human reproduction

ORIGINAL RESEARCH

Follicular hormone dynamics during the midcycle surge of gonadotropins in women undergoing fertility treatment

L.C. Poulsen [1,*], A.L.M. Englund[1], A.S. Andersen[2], J.A. Bøtkjær[2], L.S. Mamsen[2], P. Damdimopoulou[3,4], O. Østrup[5], M.L. Grøndahl[6], and C. Yding Andersen[2]

[1]Fertility Clinic, Zealand University Hospital, Lykkebækvej 14, 4600 Køge, Denmark [2]Laboratory of Reproductive Biology, University Hospital of Copenhagen, Rigshospitalet, Blegdamsvej 9, 2100 Copenhagen Ø, Denmark [3]Swedish Toxicology Sciences Research Centre (Swetox), Karolinska Institute, Unit of Toxicology Sciences, 15136 Södertälje, Sweden [4]Department of Clinical Science, Intervention and Technology, Karolinska Institute, SE-141 83 Stockholm, Sweden [5]Center for Genomic Medicine, Microarray Core Facility, Rigshospitalet, Blegdamsvej 9, 2100 Copenhagen Ø, Denmark [6]Fertility Clinic, University Hospital of Copenhagen, Herlev and Gentofte Hospital, Herlev Ringvej 75, 2730 Herlev, Denmark

*Correspondence address. E-mail: livlacour@hotmail.com orcid.org/0000-0003-1160-6924

Submitted on November 22, 2019; resubmitted on January 21, 2020; editorial decision on January 31, 2020

ABSTRACT: Changes in concentrations of intra-follicular hormones during ovulation are important for final oocyte maturation and endometrial priming to ensure reproductive success. As no human studies have investigated these changes in detail, our objective was to describe the dynamics of major follicular fluid (FF) hormones and transcription of steroidogenic enzymes and steroid receptors in human granulosa cells (GCs) during ovulation. We conducted a prospective cohort study at a public fertility clinic in 2016–2018. Fifty women undergoing ovarian stimulation for fertility treatment were included. From each woman, FF and GCs were collected by transvaginal ultrasound-guided follicle puncture of one follicle at two specific time points during ovulation, and the study covered a total of five time points: before ovulation induction (OI), 12, 17, 32 and 36 h after OI. Follicular fluid concentrations of oestradiol, progesterone, androstenedione, testosterone, 17-hydroxyprogesterone, anti-Mullerian hormone, inhibin A and inhibin B were measured using ELISA assays, and a statistical mixed model was used to analyse differences in hormone levels between time points. Gene expression of 33 steroidogenic enzymes and six hormone receptors in GCs across ovulation were assessed by microarray analysis, and selected genes were validated by quantitative reverse transcription PCR. We found that concentrations of oestradiol, testosterone, progesterone, AMH, inhibin A and inhibin B ($P < 0.001$) and gene expression of 12 steroidogenic enzymes and five receptors (false discovery rate < 0.0001) changed significantly during ovulation. Furthermore, we found parallel changes in plasma hormones. The substantial changes in follicular hormone production during ovulation highlight their importance for reproductive success.

Key words: ovulation / steroid hormones / inhibin / LH / oocyte maturation / dynamics / steroidogenic enzymes / transcription

Introduction

Hormone secretions from theca cells (TCs) and granulosa cells (GCs) are mainly regulated by gonadotropins (i.e. FSH and LH) but also by autocrine and paracrine signalling that involves inhibins, activins, follistatin and anti-Müllerian hormone (AMH) (Andersen *et al.*, 2010; Yding Andersen, 2017). These regulatory systems orchestrate the coordinated action of more than 20 steroidogenic enzymes in the ovary, ultimately securing synthesis of oestradiol and progesterone (Miller, 2008). Whereas progesterone is synthesized by both TCs and GCs, the synthesis of oestradiol requires a coordinated action of both cell types as described in the two-cell-two-gonadotropin model (Hillier *et al.*, 1994).

When the follicle is fully mature, ovulation is initiated by a massive surge of LH and FSH, which prompts resumption of oocyte maturation, rupture of the follicle wall and transformation of the follicle into the corpus luteum (CL). During ovulation, the follicle undergoes a transformation from a mainly oestrogen-producing to a mainly progesterone-producing unit. The progressive changes in the hormone concentrations, their inter-relationships and secretory regulation during the events of ovulation are important for proper hormonal stimulation of the reproductive organs, development of a receptive endometrium, oocyte maturation and ultimately reproductive success.

In humans, the detailed steroidogenic shift is exclusively documented in studies examining serum or urine steroid levels across the mid-cycle surge (Aedo *et al.*, 1981; Hoff *et al.*, 1983; Fritz *et al.*, 1992;

Roos *et al.*, 2015). Studies reporting the shift in the intra-follicular hormonal milieu that directly supports the maturing oocyte and follicle transformation are limited to animal or primate studies (Chaffin *et al.*, 1999; Belin *et al.*, 2000; Komar *et al.*, 2001). Thus, little information exists on the intra-follicular hormone milieu during ovulation in humans.

The aim of the present study was to monitor the concentrations of predominant hormones in human follicles at five specific time points over the course of ovulation and the simultaneous changes in transcription of steroidogenic enzymes and their receptors in GCs. The results increase our knowledge of the intra-follicular hormonal dynamics that support this crucial time in follicle and oocyte development.

Materials and Methods

Ethical approval

The Danish Data Protection Agency and the Scientific Ethical Committee of Region Zealand, Denmark, approved the study (SJ-530). All study participants gave informed consent prior to inclusion. The study was conducted in accordance with the Helsinki Declaration II.

Study participants

The study was conducted as a prospective cohort at the University Hospital-affiliated Fertility Clinic, Holbæk Hospital, Region Zealand, Denmark, during September 2016 to March 2018, as previously described (Poulsen *et al.*, 2019b). Included women were below 36 years of age, undergoing IVF or ICSI treatment because of infertility due to male factor, tubal factor or unexplained infertility, including six women with polycystic ovary syndrome (PCOS). For ethical reasons, only women who had developed at least nine mature follicles ≥14 mm at the last control ultrasound before ovulation induction (OI) were asked to participate. Women with elevated serum androgens and co-morbidities such as diseases of lung, heart, bowel, kidney, diabetes or dysregulated thyroid disease were excluded. The women were treated with a standard antagonist protocol initiated at cycle Day 2 or 3 with individually dosed recombinant FSH ($n = 42$, rFSH, Puregon®, MSD, Denmark) or human menopausal gonadotropin ($n = 8$, hMG, Menopur®, Ferring, Denmark) and a GnRH antagonist (ganirelix 0.25 mg, Fyremadel®, SUN Pharma, Netherlands) from stimulation Day 5. To avoid ovarian hyperstimulation syndrome (OHSS), ovulation was induced with either recombinant human chorionic gonadotropin (rhCG, 6500 IU, Ovitrelle®, Merck, Germany) or GnRH agonist (GNRHa, buserelin 0.5 mg, Suprefact®, Sanofi-Aventis, France) according to the number of ovarian follicles at the final control visit, as evaluated by ultrasound and/or early clinical signs of OHSS. Oocyte pickup (OPU) was performed 36 h after OI.

Baseline descriptive parameters

BMI and cause of infertility were recorded at the woman's first visit to the clinic when treatment was planned. At cycle Day 2 or 3, before initiation of treatment, all women had a blood sample drawn for evaluation of baseline hormone parameters: LH, FSH, oestradiol, AMH, prolactin and thyroid stimulating hormone (TSH). Serum androgens were measured in a blood sample collected just prior to the follicular fluid (FF) sampling described below. All serum hormone analyses were performed as routine analyses at the hospital's biochemical laboratory. At the final control ultrasound before OI, the number of mature follicles was counted. Follicles with a diameter of ≥14 mm, measured as an average of two orthogonal planes, were considered mature.

Follicle punctures

FF and GCs were collected from four groups of women by aspiration of one mature follicle: before OI (Group 1, '0 h', $n = 23$)), 12 h after OI (Group 2, '12 h', $n = 10$), 17 h after OI (Group 3, '17 h', $n = 6$) and 32 h after OI (Group 4, '32 h', $n = 11$). From each of these women, a FF sample was also collected at OPU ('36 h', $n = 50$). Consequently, each woman contributed with two samples of FF and GCs (repeated measurements), and the study covered a total of five sample time points during the 36 h of ovulation (Fig. 1).

Sample collection was performed by transvaginal ultrasound-guided follicle puncture with a single lumen needle (Wallace Oocyte Recovery Set, Smith Medical, Australia). Samples collected prior to OPU (0–32 h) were aspirated from one easily accessible follicle of at least 14 mm with subsequent double flushing to retrieve additional GCs. Samples at OPU (36 h) were collected from the first aspirated follicle containing a cumulus–oocyte complex, where double flushing was performed in between different follicle aspirations to prevent inter-follicle contamination and increase the number of available GCs. Therefore, FF collected at OPU was in some cases diluted with precisely 1.5 mL of flushing medium (ASP®, 10 100, Vitrolife, Sweden) contained in the needle system. This volume was accounted for by determining the dilution factor for each case ((follicle volume + flush volume)/follicle volume), which was used to correct the measured FF hormone concentrations.

Isolation of GCs and FF

Through a light microscope, flakes of GCs were isolated from the aspirated FF with a 100-µL pipette while visible red blood cells and blood clots were avoided. The cells were washed through a 4-well dish containing phosphate-buffered saline (PBS) and 0.1% polyvinyl alcohol (PVA) (Sigma-Aldrich, Denmark), transferred to a 0.2-mL cryotube (MicroAmp, Applied Biosystems, CA, USA) with minimal PBS and snap-frozen in liquid nitrogen. The tubes were stored at −80°C within 30 min after follicle puncture.

The volume of the aspirated follicle was determined by stepwise measurement of the aspirated FF with 500- and 100-µL pipettes, and for first punctured follicles an addition of the 1.5 mL contained in the needle system (follicle volume = aspirated volume + 1.5 mL). The FF was centrifuged at 300*g* for 10 min to remove cell debris, and the supernatant was collected and stored in cryovials (1.5 mL, NUNC, Fisher Scientific, Denmark) at −80°C until further analyses. All samples were macroscopically clear or contained only trace amounts of blood.

Plasma samples

Within 30 min before both the follicle puncture and OPU, a blood sample was collected from each woman. The sample was collected in an EDTA tube, centrifuged at 2000*g* for 20 min, and the supernatant was collected and stored in cryovials (1.5 mL, NUNC, Fisher Scientific, Denmark) at −80°C until further analyses.

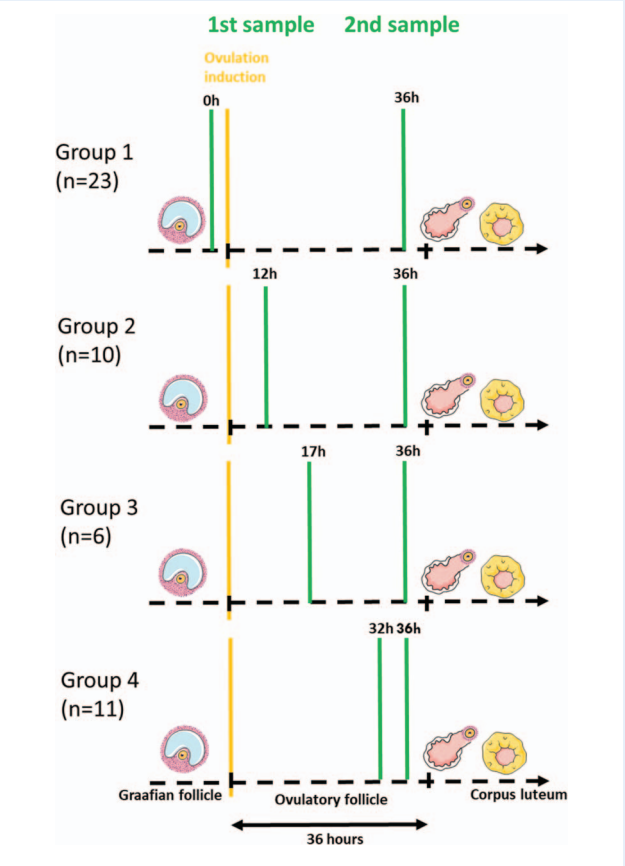

Figure 1 Study groups. The sampling time defined four groups of patients to cover five study time points in total. Each patient gave consent to donate the content of one follicle at one specific time point before oocyte pickup (0–32 h) as well as granulosa cells and follicular fluid from one follicle at oocyte pickup (36 h). The yellow vertical line indicates ovulation induction, and the green vertical lines the sampling time points. The figure was created with Servier Medical Art under the CC BY 3.0 licence.

Enzyme-linked immunosorbent assays

In FF, concentrations of five steroid hormones were measured using commercially available ELISA kits: 17-beta-oestradiol, progesterone, testosterone and androstenedione (DNOV003, DNOV006, DNOV002 and DNOV008, respectively, NovaTec Immundiagnostica, Germany), and 17-hydroxyprogesterone (RE52071, IBL International, Germany). Concentrations of the peptide hormones AMH, inhibin A and inhibin B were measured using special ELISA kits (AL-105-i, AL-123-i and AL-107-I, respectively, Ansh Labs, TX, USA). All ELISAs were performed according to the manufacturers' instructions. Intra- and interassay variations and cross-reactivity towards other steroids are listed in Supplementary Table SI. Prior to analysis, FF was diluted in PBS with 1% bovine serum albumin (BSA). Testosterone, androstenedione and AMH were diluted 1:10, progesterone, 17-hydroxyprogesterone and oestradiol 1:2000, and inhibins 1:200 or 1:2000 at low and high concentrations, respectively. Samples with concentrations below the lower detection limit were assigned the value of the lower detection limit (12 out of 100 for testosterone, 8 out of 100 for progesterone, while the remaining had 100% valid values).

To monitor the relationship between intra-follicular and circulating hormone levels, concentrations of oestradiol, progesterone, testosterone, androstenedione, inhibin A and inhibin B were measured in the collected plasma samples using the same ELISAs described above. For oestradiol measurements, plasma samples were diluted 1:5 in PBS with 1% BSA, and for inhibins they were diluted 1:50. For testosterone, 80 out of 100 samples were below the detection limit of the assay (<0.1 ng/mL), and this steroid was therefore excluded from further analyses. Valid values were measured in 100% of samples for the remaining hormones.

The performance of the steroid ELISAs in FF was validated by ultra performance liquid chromatography mass spectrometry (UPLC-MS) at Swetox, Karolinska Institutet, Unit of Toxicological Sciences, Södertälje, Sweden, as described previously (Hao *et al.*, 2018). Details of FF samples used for the validation are available in Supplementary Methods. Highly significant correlation R^2 values ($P < 0.001$) confirming a significant linear correlation between the two assays were obtained for oestradiol ($R^2 = 0.7447$), progesterone ($R^2 = 0.4628$), testosterone ($R^2 = 0.5516$) and androstenedione ($R^2 = 0.4742$). The slopes of the linear correlations were below 1, showing that the ELISAs measured a higher concentration as compared to the UPLC-MS assay.

Microarray analyses

Total RNA was isolated from the GCs using the Arcturus PicoPure® RNA Isolation Kit (Applied Biosystems, CA, USA) according to the manufacturer's instructions. NanoDrop (Thermo Fisher, MA, USA) and Bioanalyzer RNA 6000 Pico Kit (Agilent, SC, USA) were used to assess quality and quantity of purified RNA. The amount of total RNA per sample ranged from 0.19 to 286 ng/μL. For details, see Supplementary Table SII.

Based on concentration and RNA integrity number (RIN), RNA was subsequently processed using Clariom D™ Pico Assay (Applied Biosystems, Thermo Fisher, MA, USA) according to the manufacturer's protocol. The arrays were washed and stained with phycoerythrin conjugated streptavidin using the Affymetrix Fluidics Station 450, and the arrays were scanned in the Affymetrix GeneArray 3000 7G scanner to generate fluorescent images. Cell intensity files (.CEL files) were generated in the GeneChip Command Console Software (AGCC, Affymetrix, Thermo Fisher, USA). Seventeen out of 100 samples were excluded from further analysis because of either insufficient RNA or bad quality of RNA resulting in outliers. The 83 CEL files, representing time points 0 h ($n = 17$), 12 h ($n = 7$), 17 h ($n = 6$), 32 h ($n = 9$) and 36 h ($n = 44$), were processed in Transcriptome Analysis Console (TAC 4.0.1, Thermo Fisher Scientific, MA, USA) where data summarization, quantile normalization, gene summaries and statistical analysis were performed in one analysis flow. Summarization and normalization were performed by the SST-RMA approach (signal space transformation—robust multi-array average), which is standard in TAC to optimize fold changes compared to RMA alone (Bolstad *et al.*, 2003; Affymetrix, 2019).

The differential expression analysis was set up using ANOVA eBayes comparisons with an advanced random factor for 'patient ID', accounting for the pairing of samples. Differential expression with a false discovery rate (FDR) < 0.01 combined with a gene expression fold change > 2 was considered significant. Raw and processed microarray

data were deposited to the Gene Expression Omnibus (www.ncbi.nlm.nih.gov/geo, accession number: GSE133868).

Expression of leukocyte-specific marker *PTPRC* (CD45) was consistently very low across time points indicating no or low leukocyte contamination with no differences between time points. Similarly, large or unequal TC contamination of the GC samples was found unlikely as TC markers such as insulin-like 3 (*INSL3*) and actin 2 gamma (*ACTG2*) showed consistently low expression across the time points (Supplementary Table SIII).

For the present study, only steroidogenic enzymes and steroid receptors were evaluated to support the hormone analyses. The remaining microarray data is described in a different report (Poulsen *et al.* unpublished data). A list of 33 genes of importance to steroid production and six genes encoding hormone receptors was extracted from the microarray dataset (Supplementary Table SIII). A heatmap and dendrogram of differentially expressed genes with FDR < 0.0001 was produced with Morpheus (www.software.broadinstitute.org/morpheus, Broad Institute, MA, USA).

Validation of microarray results

The microarray data was validated by predesigned TaqMan™ gene expression assays (Thermo Fisher Scientific, MA, USA) of 5 selected genes: cytochrome P450 family 19 subtype A1 (*CYP19A1,* also known as aromatase*),* steroid acute regulatory protein *(STAR),* 3β-hydroxysteroid dehydrogenase 2 (*HSD3B2),* 17β-hydroxysteroid dehydrogenase 1 *(HSD17B1)* and 11β-hydroxysteroid dehydrogenase 1 (*HSD11B1)* (product numbers: Hs00903411_m1, Hs00264912_m1, Hs00605123_m1, Hs00166219_g1 and Hs01547870_m1, respectively). The samples were prepared in duplicates with TaqMan™ Fast Advanced Master Mix (catalog no. 4444557, Thermo Fisher Scientific, MA, USA) according to the manufacturer's instructions. Gene expression was normalized to glyceraldehyde 3-phosphate dehydrogenase (*GAPDH,* Hs02786624_g1), because this gene has been shown to be highly and stably expressed across follicle classes (Kristensen *et al.*, 2014), as well as in the present ovulatory microarray dataset. PCR expression was evaluated at selected time points: 0 h (n = 17), 12 h (n = 6) and 32 h (n = 8) (*HSD3B2, STAR, HSD17B1, HSD11B1*), and 17 h and 36 h (n = 5, paired samples; *CYP19A1*). Selected time points were used due to sparse material. The specific genes were selected to validate different expression profiles. Validation was performed on the same samples as the microarray analysis, thus representing technical validation. Validation in a larger cohort was not possible due to considerable difficulty in obtaining the samples.

Statistical analyses

All tests described in this section were performed with SPSS (v25, IBM, NY, USA). Unless otherwise mentioned, $P < 0.05$ was considered significant.

Continuous baseline descriptive parameters were compared with a Kruskal–Wallis test followed by *post hoc* test with a Bonferroni correction as a normal distribution could not be assumed and because study groups were of unequal size. Categorical parameters were compared by Fisher's exact test.

All FF and plasma hormone concentrations were log-transformed to ensure a normal distribution prior to statistical modelling. To account for the patient-factor in our pairwise repeated measurements design, differences in concentrations between time points were analyzed by a mixed model with 'patient-ID' as a random factor and 'time' as a repeated, fixed factor using the first order autoregressive (AR(1)) covariance matrix as this resulted in the best model fit. For all measured hormones, it was tested whether choice of treatment or ovulation trigger had a significant effect on the measured concentration, and if a significant effect was found, the final model was adjusted by adding the parameter as a fixed factor. A *post hoc* test with Bonferroni correction was used to test differences between the resulting estimated marginal (EM) means at each time point.

Correlations between the log-transformed FF hormone concentrations at each of the different time points were tested in a correlation matrix. A significant correlation was defined by Pearson's correlation coefficient (R) > 0.5 or $R < -0.5$ and $P < 0.05$.

Differential qRT-PCR gene expression was assessed by a Kruskal–Wallis test for genes compared between time points 0, 12 and 32 h, and by a paired t-test for genes compared at time points 17 and 36 h (the latter represents women with repeated measurements).

Results

Baseline parameters

Baseline descriptive parameters were similar across the four groups except for four parameters (Table I): plasma sex hormone binding globulin (SHBG) was significantly lower and BMI significantly higher in Group 1 compared to Group 4, while the size of the aspirated follicles were significantly larger at 32 h compared to 0 h. The fraction of patients with male factor infertility was higher in Group 1. The duration between OI and FF aspiration was very close to the designated time points at 12, 17, 32 and 36 h. For 0-h samples, however, aspiration of FF was allowed up to 2 days before OI (on the day of OI (n = 16), the day before OI (n = 6) or 2 days before OI (n = 1)). There were no apparent or statistical differences in the FF hormone concentrations between these three '0 h'-groups, except for inhibin B which decreased slightly towards OI (Supplementary Fig. S1).

Intra-follicular hormone levels

All measured FF hormones were significantly regulated across ovulation except for androstenedione and 17-hydroxyprogesterone (Table II, Fig. 2). The FF progesterone concentration increased rapidly after OI to peak with a mean concentration of 38.2 µg/mL at 17 h. While progesterone and 17-hydroxyprogesterone showed approximately similar concentrations at 0 h, 17-hydroxyprogesterone showed negligible increase with a 20-fold lower concentration at 17 h compared to progesterone. Intra-follicular oestradiol levels peaked before OI with a mean concentration of 2323 ng/mL and decreased throughout the course of ovulation. Testosterone followed the same decreasing pattern as oestradiol at much lower concentrations with a peak mean concentration at 0 h of 19.5 ng/mL, while androstenedione presented mean levels of 7–11 ng/mL across the study time points. Intra-follicular Inhibin A and B concentrations showed two distinct patterns: inhibin A increased to peak at 17 h with a mean concentration of 264 ng/mL and subsequently decreased, whereas inhibin B had the highest concentration at 0 h of 369 ng/mL and decreased significantly after 17 h. AMH decreased significantly in FF from 12 to 32 h with

Table I Baseline descriptive parameters.

Parameter		Group 1 0 h + 36 h (N = 23)	Group 2 12 h + 36 h (N = 10)	Group 3 17 h + 36 h (N = 6)	Group 4 32 h + 36 h (N = 11)	P value
Cause of infertility (distribution in numbers)	Male factor	17	6	2	7	0.016**
	Tubal factor	4	0	1	0	
	Unexplained	0	4	1	2	
	PCOS	2	0	2	2	
Duration between OI and FF collection early puncture (hours)		−11.9 (22.6)	12.0 (0.2)	17.0 (0.2)	32.3 (0.2)	-
Duration between OI and FF collection at OPU (hours)		36.0 (0.1)	36.0 (0.2)	36.3 (0.2)	36.1 (0.2)	-
Age (years)		28.5 (4.9)	28.0 (4.2)	28.8 (7.1)	27.9 (3.5)	NS
BMI		24.8 (5.0)*	21.8 (3.8)	21.9 (4.7)	21.6 (2.4)*	0.026
Stimulation dosage, total (IU)		1437 (487)	1350 (388)	1275 (1019)	1200 (418)	NS
Number of follicles at last control visit		12 (4)	11.5 (3.3)	14 (6)	14 (6)	NS
Size of aspirated follicle 0–32 h (mL)		3.1 (2.2)*	3.7 (2.1)	3.7 (2.7)	6.8 (3.9)*	0.001
Size of aspirated follicle 36 h (mL)		4.5 (3.9)	4.3 (3.1)	3.6 (3.7)	5.2 (2.5)	NS
S-LH (IU/L)		4.1 (2.7)	4.7 (2.3)	5.6 (2.4)	5.5 (2.2)	NS
S-FSH (IU/L)		5.2 (2.3)	6.6 (2.6)	5.6 (2.9)	6.5 (2.2)	NS
S-Prolactin (mU/L)		226 (98)	213 (132)	191 (106)	172 (57)	NS
S-TSH (mU/L)		1.7 (0.6)	1.4 (0.8)	1.3 (1.5)	1.8 (1.0)	NS
S-SHBG (nmol/L)		117 (89)*	166 (94.8)	132 (28)	167 (45)*	0.038
S-Testosterone, free fraction (nmol/L)		0.019 (0.009)	0.020 (0.011)	0.020 (0.004)	0.015 (0.016)	NS
S-DHEAS (μmol/L)		5.9 (2.3)	5.7 (3.5)	5.4 (2.3)	5.4 (2.4)	NS
S-Oestradiol (nmol/L)		0.10 (0.05)	0.16 (0.08)	0.12 (0.05)	0.14 (0.10)	NS
S-AMH (pmol/L)		33.9 (22.7)	30.3 (29.3)	28.1 (35.2)	25.6 (21.2)	NS

Median (interquartile range) is reported. The differences between the groups were compared by Kruskal–Wallis' test followed by a *post hoc* test with Bonferroni correction if a difference was detected. $P < 0.05$ was considered significant. *Post hoc test showed a difference between the marked groups. **Fisher's exact test showed a difference due to a higher number of MF in group 1, whereas no differences were found between the remaining groups. NS = non-significant, PCOS: non-hyperandrogenic polycystic ovary syndrome, OI: ovulation induction, FF: follicular fluid, OPU: oocyte pickup, TSH: thyroid stimulating hormone, SHBG: sex hormone binding globulin, DHEAS: dihydroepiandrostenedione, AMH: anti-Müllerian hormone.

concentrations ranging from 2.4 to 6.7 ng/mL. The statistical models were adjusted for effects of treatment and triggering as described in the Materials and Methods section. We found an overall significant positive effect of hMG-treatment compared to rFSH treatment for FF androstenedione ($P = 0.001$), testosterone ($P = 0.014$) and inhibin B ($P = 0.023$) and borderline significant differences for FF AMH and oestradiol (Table II). Likewise, we found a significant positive effect of rhCG-triggering compared to agonist triggering for FF progesterone ($P = 0.001$) and 17-hydroxyprogesterone ($P = 0.028$). The significant regulation across time was unaffected by adjustments for treatment.

Furthermore, the significant regulation across time was not affected by adjustment for follicle size, SHBG or BMI (factors with unequal group distribution in the baseline parameters). The six non-hyperandrogenic PCOS women that were included did not appear to have higher FF androgen concentrations at any time point compared to patients with other causes of infertility (Supplementary Fig. S2). At 36 h, this was tested by a Kruskal–Wallis test, which showed no significant difference (data not shown).

The correlation analysis showed significant positive correlations between FF, testosterone and oestradiol at 12, 32 and 36 h. A similar positive correlation was found between FF testosterone and androstenedione at 0, 32 and 36 h and FF oestradiol and androstenedione at 12 and 17 h. Furthermore, FF progesterone and 17-hydroxyprogesterone were positively correlated at 0 h, and inhibin B was negatively correlated with both of them at 0 h and with 17-hydroxyprogesterone at 17 h (Fig. 3).

Circulating hormone levels

The plasma hormone levels mostly mirrored the FF hormone concentrations (Fig. 4 and Supplementary Table SIV). Plasma oestradiol decreased throughout ovulation, while androstenedione showed no significant changes. Both plasma progesterone and 17-hydroxyprogesterone increased significantly to peak at 17 h, but the subsequent decrease was only significant for 17-hydroxyprogesterone. Plasma inhibin A showed a significant peak at 17 h and inhibin B decreased significantly after 17 h. The ratios between the FF concentration and the circulating concentration were unique to each hormone, but relatively constant across ovulation for all measured hormones, except progesterone: at 0 h, the plasma to FF ratio for progesterone was 1:500, and at 17 h, it was 1:2000.

Table II **Levels of follicular fluid hormones during ovulation.**

Measured parameter	Time point level					Time effect *P* value	Significant regulation	Treatment effect hMG vs rFSH		Trigger effect rhCG vs GNRHA	
	0 h *N* = 23	12 h *N* = 10	17 h *N* = 6	32 h *N* = 11	36 h *N* = 50		*Post hoc* test	Difference ng/mL	*P* value	Difference µg/mL	*P* value
Progesterone (µg/mL)	1.3 (1.0;1.8)	12.6 (8.0;19.8)	38.2 (21.7;67.1)	20.2 (13.4;30.5)	13.6 (11.1;16.6)	<0.001	0–12 h; 0–17 h; 0–32 h; 0–36 h; 12–17 h; 17–36 h		0.132	1.7 (1.2;2.2)	0.001
17-Hydroxyprogesterone (µg/mL)	1.2 (0.9;1.4)	1.9 (1.3;2.7)	2.1 (1.4;3.1)	1.6 (1.2;2.1)	1.4 (1.2;1.6)	0.038	-		0.602	1.3 (1.03;1.7)	0.028
Oestradiol (ng/mL)	2322.7 (1733.8;3118.9)	1606.9 (1025.7;2517.7)	1492.8 (895.4;2488.9)	1099.0 (785.2;1541.7)	599.8 (487.5;737.9)	<0.001	0–32 h; 0–36 h; 12–36 h; 17–36 h; 32–36 h		0.060		0.542
Testosterone (ng/mL)	19.5 (13.5;28.1)	7.1 (4.1;12.2)	6.5 (3.6;11.6)	5.6 (3.7;8.6)	3.6 (2.6;4.9)	<0.001	0–12 h; 0–17 h; 0–32 h; 0–36 h	2.1 (1.2;3.8)	0.014		0.790
Androstenedione (ng/mL)	8.2 (6.8;10.0)	8.2 (6.0;11.3)	11.1 (7.7;16.0)	7.3 (5.7;9.5)	7.6 (6.5;8.9)	0.278	-	1.6 (1.2;2.1)	0.001		0.344
AMH (ng/mL)	6.2 (4.6;8.3)	6.7 (4.5;9.8)	4.3 (2.9;6.5)	2.4 (1.8;3.2)	3.6 (2.9;4.5)	<0.001	0–32 h; 0–36 h; 12–32 h; 12–36 h; 32–36 h		0.080		0.431
Inhibin A (ng/mL)	119.9 (102.8;140.3)	195.0 (154.2;246.6)	263.6 (200.9;346.7)	141.3 (117.8;169.4)	110.4 (99.3;122.7)	<0.001	0–12 h; 0–17 h; 12–36 h; 17–32 h; 17–36 h		0.612		0.593
Inhibin B (ng/mL)	369.0 (272.3;501.2)	229.6 (141.6;372.4)	325.1 (190.1;555.9)	106.4 (73.1;155.2)	95.3 (74.1;122.7)	<0.001	0–32 h; 0–36 h; 12–36 h; 17–32 h; 17–36 h	1.7 (1.1;2.7)	0.023		0.276

Results from the statistical mixed model. All parameters were modelled with the first order autoregressive (AR(1)) covariance matrix. The model was adjusted for treatment or trigger if the parameter effect was significant. Estimated marginal means and 95% confidence intervals for each time point are reported. Significant regulation was defined as *P* value. 0 h: before ovulation induction (OI), 12 h: 12 h after OI, 17 h: 17 h after OI, 32 h: 32 h after OI, 36 h: 36 h after OI. Treatment effect: test for overall difference caused by stimulation drug. Trigger effect: test for overall difference caused by trigger drug. hMG: human menopausal gonadotropin. rFSH: recombinant follicle stimulating hormone. rhCG: recombinant human chorionic gonadotropin. GnRHa: gonadotropin releasing hormone agonist.

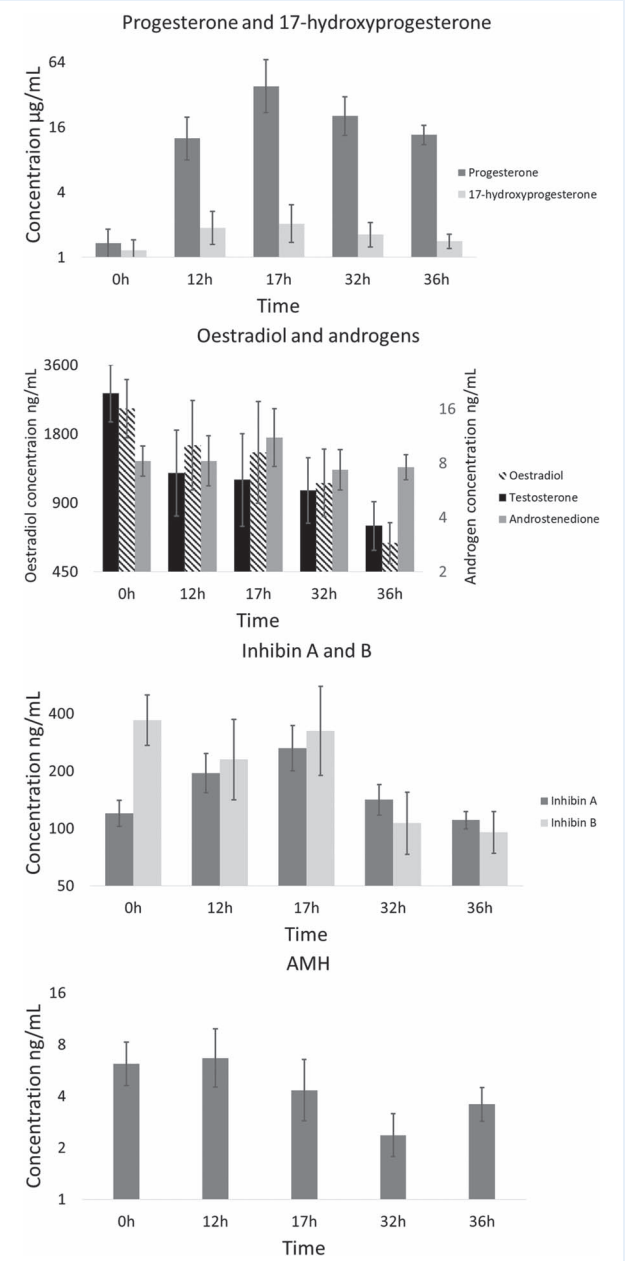

Figure 2 Mean follicular fluid hormone concentration across ovulation. Estimated marginal means and error bars (95% confidence intervals) for each time point are depicted on a log *y*-axis. 0 h: before ovulation induction (OI), 12 h: 12 h after OI, 17 h: 17 h after OI, 32 h: 32 h after OI, 36 h: 36 h after OI. Significant changes: progesterone (0–12 h; 0–17 h; 0–32 h; 0–36 h; 12–17 h; 17–36 h), 17-hydroxyprogesterone (none), oestradiol (0–32 h; 0–36 h; 12–36 h; 17–36 h; 32–36 h), testosterone (0–12 h; 0–17 h; 0–32 h; 0–36 h), androstenedione (none), inhibin A (0–12 h; 0–17 h; 12–36 h; 17–32 h; 17–36 h), inhibin B (0–32 h; 0–36 h; 12–36 h; 17–32 h; 17–36 h), AMH (anti-Müllerian hormone) (0–32 h; 0–36 h; 12–32 h; 12–36 h; 32–36 h).

Gene expression

The microarray analysis on aspirated GCs showed that 12 genes of importance for steroid production were significantly regulated during ovulation (FDR < 0.0001) (Fig. 5, Supplementary Table SIII). Seven of these genes increased to peak at 12-17 h after OI: *STAR*, *HSD3B1*, *HSD3B2*, *HSD17B12*, *HSD17B6*, *CYP11A1* and *AKRC1*, of which *STAR*, *HSD3B2* and *CYP11A1* were highly expressed. Four genes were at their highest level at 0 h before decreasing: *CYP19A1*, *CYP17A1*, *HSD17B1* and *HSD11B2*. In contrast, *HSD11B1* increased remarkably 0–17 h and stayed elevated throughout the remaining time points. Five of the six studied hormone receptors were significantly regulated (FDR < 0.0001). Genes encoding the oestrogen receptor 2 (*ESR2*), androgen receptor (*AR*) and AMH receptor 2 (*AMHR2*) decreased significantly after OI. The progesterone receptor (*PGR*) expression increased substantially from 0 to 17 h with a rapid subsequent decrease. The glucocorticoid receptor encoded by *NR3C1* showed an intermediate peak at 12–17 h and a similar peak at 36 h.

Technical qRT-PCR validation of five selected genes was consistent with the microarray findings with similar expression patterns for all examined genes and significant regulation of four out of five genes (Supplementary Fig. S3).

Discussion

This descriptive study determines for the first time in detail the dynamic changes in the hormonal milieu and transcription of steroidogenic enzymes in human follicles during the course of ovulation. We measured important ovarian steroid and peptide hormones in human follicles at five different time points: before OI, and 12, 17, 32 and 36 h after OI, capturing the period from initiation of the midcycle surge of gonadotropins until follicle rupture. The hormone dynamics are supported by changes in transcription of steroidogenic enzymes. We observed a decrease in sex steroids downstream of CYP17A1 (testosterone and oestradiol) and a reduced capacity for conversion of androgens to oestradiol as both *CYP19A1* and *HSD17B1* decreased in GCs after OI. In contrast, the progesterone concentration increased substantially and peaked at 17 h after OI, paralleled by a peak in gene expression of *STAR*, *CYP11A1* and *HSD3B2* at 12–17 h after OI. The production of cortisol, a steroid that likely plays a vital role in the anti-inflammatory system that constrains the inflammatory process associated with ovulation, acting through the upregulated nuclear glucocorticoid receptor (*NR3C1*) (Andersen, 2002; Poulsen *et al.*, 2019a), was evident by dramatic changes in *HSD11B1* and *HSD11B2*. We showed significant regulation of steroid receptors in GCs, which designates specific intra-follicular roles for the steroids, acting on the GCs, as outlined in the sections below.

Our study showed that progesterone synthesis from pregnenolone during ovulation could be a result of both HSD3B1 and HSD3B2 activity, as the genes encoding these enzymes were both expressed and significantly regulated in GCs with a peak at 12–17 h after OI. Previously, HSD3B1 has primarily been ascribed a role in the placenta (Fagerberg *et al.*, 2014). The increased production of progesterone following the LH surge is well established, as are its pivotal functions for subsequent implantation and pregnancy (American Society for Reproductive Medicine (ASRM) Practice Committee, 2012). However, the present study documents for the first time that human intra-follicular progesterone concentrations peak during ovulation around 17 h after OI. A previous report from rhesus monkeys undergoing ovarian stimulation found that progesterone peaked at 12 h and plateaued thereafter (Chaffin *et al.*, 1999), which may be due to their lack of sampling

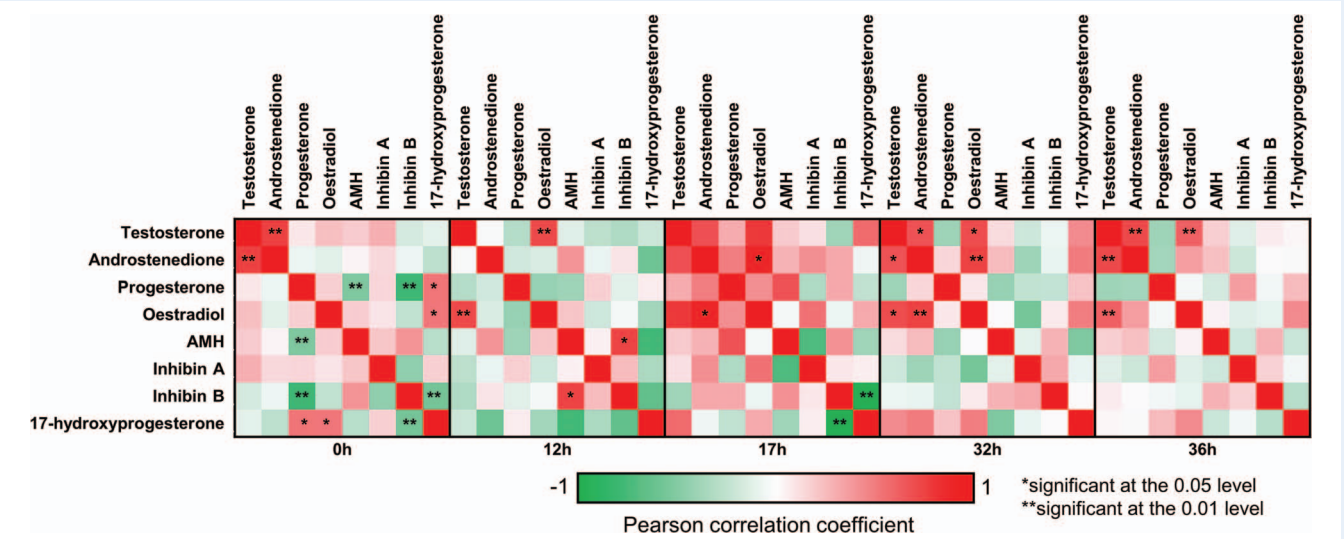

Figure 3 Correlations between measured follicular fluid hormones at individual time points. Pearson's correlation coefficients between −1 (perfect negative correlation) and 1 (perfect positive correlation) are depicted. $R > 0.5$ or < -0.5 with $P < 0.05$ was considered significant.

between 12 and 24 h. As observed in the present study, a massive peak in *PGR* expression accompanied the mid-ovulatory progesterone peak. This enforces that progesterone serves to initiate important GC signalling cascades during the ovulatory process. Our data support a previous finding where *PGR* was upregulated to peak in human GCs *in vivo* between 12 and 18 h after OI and was shown to be involved in induction of prostaglandin and epidermal growth factor system mRNA synthesis (Choi *et al.*, 2017). Furthermore, studies in *PGR* knockout mice and monkeys have suggested a role for progesterone in follicle rupture, possibly by induction of metallopeptidases, while oocyte maturation is unaffected (Hibbert *et al.*, 1996; Robker *et al.*, 2000; Bishop *et al.*, 2016). The mid-ovulatory peak in progesterone may also play an extra-follicular role in terminating the LH surge by some yet unknown negative feedback mechanism (Dafopoulos *et al.*, 2006; Messinis *et al.*, 2014).

The high increase in FF progesterone but not 17-hydroxyprogesterone observed in the present study supports that there is no or little conversion of progesterone to 17-hydroxyprogesterone by CYP17A1 following OI. Furthermore, this is supported by a positive correlation between progesterone and 17-hydroxyprogesterone only at 0 h, which suggests that prior to OI, their productions are intimately connected, while after OI, their productions are detached. This may be explained by the vast increase in *HSD3B* transcription in GCs following OI, which greatly enhances progesterone production in GCs without an associated CYP17A1 conversion. CYP17A1 has, in previous studies, been shown to be strictly located to TCs in small antral follicles (Smyth *et al.*, 1993; Conley, 1994; Katulski *et al.*, 1998; Pelletier *et al.*, 2001). In contrast, the present GC gene expression showed relatively high levels of *CYP17A1* at 0 h, which decreased immediately thereafter. Therefore, our data could suggest that preovulatory GCs, just before the LH surge (in contrast to the small antral GCs), possess some capacity for 17-alpha-hydroxylation, which diminishes after OI.

Testosterone is synthesized from androstenedione by HSD17B. The activity of this conversion in the present study was supported by a strong correlation between androstenedione and testosterone at most study time points (Fig. 3). Two HSD17B subtypes are known to catalyse conversion of androstenedione to testosterone in humans: HSD17B5 (encoded by *AKR1C3*) may be the enzyme catalysing this conversion in the follicle and CL (Pelletier *et al.*, 1999; Nelson *et al.*, 2001), while HSD17B3 is primarily functional in testis (Nelson *et al.*, 2001). The present study support that the two-cell system for oestradiol production is intact during ovulation, as the GC gene expression analysis showed very low expression of both *HSD17B3* and *AKR1C3* in GCs and no differential regulation throughout ovulation (Supplementary Table SIII), which supports that the androstenedione to testosterone conversion takes place in TCs. At the same time, our data confirm that the GCs are responsible for oestradiol production, as *HSD17B1* and *CYP19A1* were highly expressed at 0 h. *HSD17B1* is only involved in conversion of oestrone to oestradiol in humans (Ghersevich *et al.*, 1994; Hillier *et al.*, 1994; Andersson and Moghrabi, 1997; Miller, 2008; Hakkarainen *et al.*, 2015), while *CYP19A1* converts testosterone to oestradiol and is also known to be strictly located to GCs (Tamura *et al.*, 1992; Whitelaw *et al.*, 1992). The GC gene expression in the present study showed decreasing activity of both routes in GCs as ovulation progressed.

The decreasing levels of oestradiol in both FF and plasma following OI confirms previous studies of circulating oestradiol, which have shown a peak just before the mid-cycle LH surge and a subsequent decrease (Aedo *et al.*, 1981; Hoff *et al.*, 1983; Fritz *et al.*, 1992; Groome *et al.*, 1996). In contrast, studies in rhesus monkeys have shown that levels of oestradiol in both FF and serum increase for 6–12 h following OI (Schenken *et al.*, 1985; Chaffin *et al.*, 1999), which indicates that there may be a discrepancy between monkey and human periovulatory oestradiol production. However, future studies are needed to confirm our findings. In the present study, *ESR2* expression decreased rapidly following OI, indicating a diminishing intra-follicular role for oestradiol. A recent study found that oestrogen and ESR2 were involved in maintaining oocyte meiotic arrest through the natriuretic peptide C and

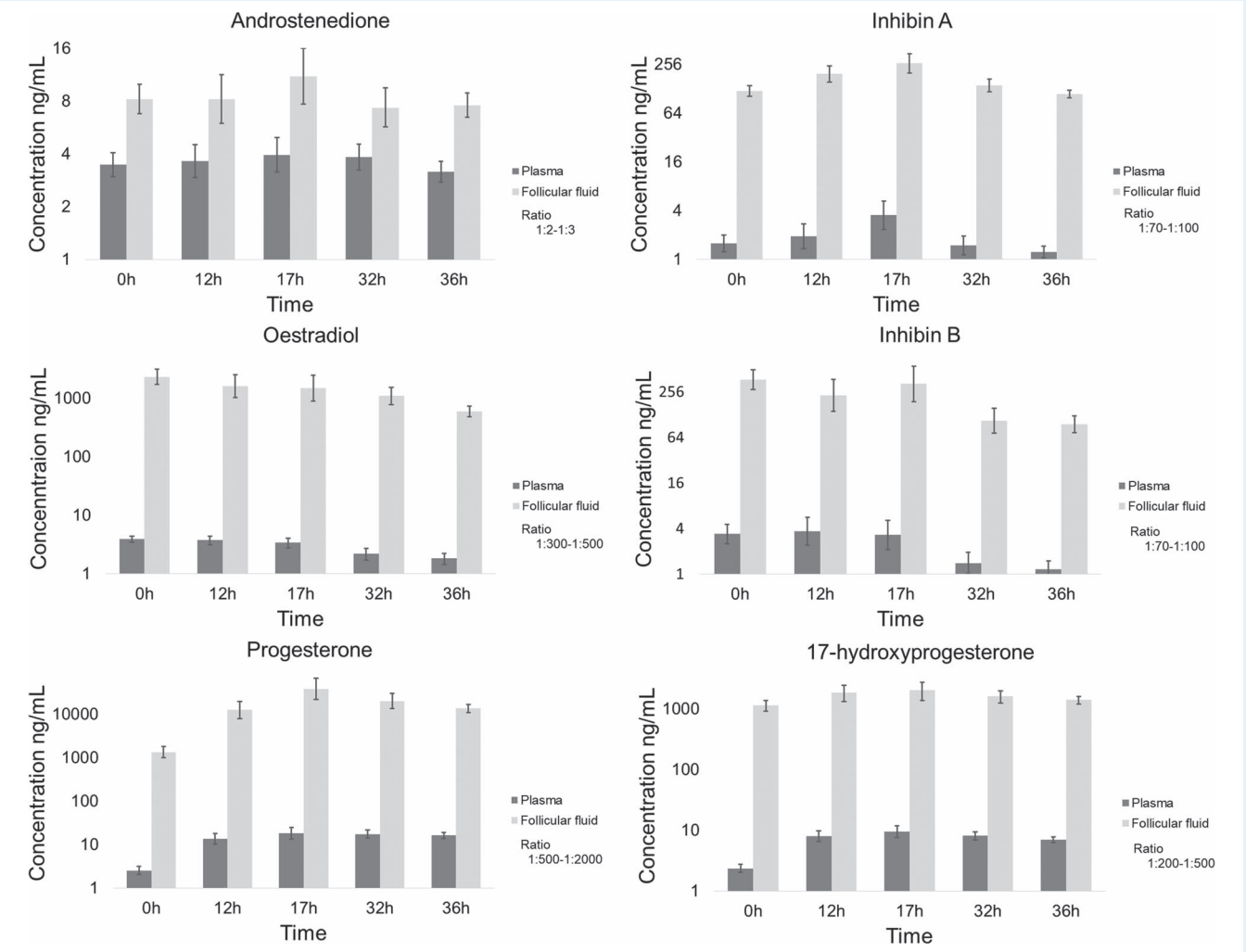

Figure 4 Mean hormone concentration across ovulation measured in follicular fluid and plasma. Estimated marginal means and error bars (95% confidence intervals) for each hormone are depicted on a log y-axis. *Significant changes in follicular fluid*: progesterone (0–12 h; 0–17 h; 0–32 h; 0–36 h; 12–17 h; 17–36 h), 17-hydroxyprogesterone (none), oestradiol (0–32 h: 0–36 h; 12–36 h; 17–36 h; 32–36 h), androstenedione (none), inhibin A (0–12 h; 0–17 h; 12–36 h; 17–32 h; 17–36 h), inhibin B (0–32 h; 0–36 h; 12–36 h; 17–32 h; 17–36 h). *Significant changes in plasma*: progesterone (0–12 h; 0–17 h; 0–32 h; 0–36 h), 17-hydroxyprogesterone (0–12 h; 0–17 h; 0–32 h; 0–36 h; 17–36 h), oestradiol (0–32 h; 0–36 h; 12–32 h; 12–36 h; 17–36 h), androstenedione (none), inhibin A (0–17 h; 17–32 h; 17–36 h), inhibin B (0–32 h; 0–36 h; 12–32 h; 12–36 h; 17–32 h; 17–36 h). Ratio values indicate plasma concentration: follicular fluid concentration ratios.

natriuretic peptide receptor 2-system (Liu *et al.*, 2017), which suggests that diminishing oestradiol levels could be one of the prerequisites for resumption of oocyte maturation.

This study documents for the first time intra-follicular inhibin concentrations during the course of ovulation. In human small antral follicles, inhibin B concentrations have been measured at 180–200 ng/mL and inhibin A levels at 40 ng/mL at a follicle diameter of 10–12 mm (Yding Andersen, 2017; Kristensen *et al.*, 2018). The present results showed that FF inhibin B levels peak prior to the LH surge and decrease significantly after 17 h, while a significant peak of inhibin A takes place at 17 h, resulting in very high collective inhibin concentrations at 17 h (588 ng/mL in FF) that has never before been documented in human FF. Furthermore, these dynamic changes were reflected in the plasma samples, and this ovulatory pattern confirms previous studies (Groome *et al.*, 1996; Lockwood *et al.*, 1996; Lee *et al.*, 2010). The high intra-follicular concentration of inhibins during the mid-ovulatory period may enhance oocyte meiotic maturation (Alak *et al.*, 1996) or induce androgen synthesis in TCs to increase libido during the fertile window (Yding Andersen, 2017), whereas the corresponding increase in circulation may serve to feedback-inhibit the ovulatory FSH surge. Furthermore, negative correlations between FF inhibin B and both progesterone and 17-hydroxyprogesterone only at 0 h (Fig. 3) may reflect that inhibin B enhance *CYP17A1* expression favouring the delta 5-pathway in expense of the delta 4-pathway thereby inhibiting progesterone production as shown before (Hillier *et al.*, 1994; Nahum *et al.*, 1995) (Fig. 6). At 17 h, inhibin B was still negatively correlated with 17-hydroxyprogesterone but not progesterone, suggesting that the effect of inhibin B is continuously exerted in TCs, while progesterone production accelerates freely in GCs.

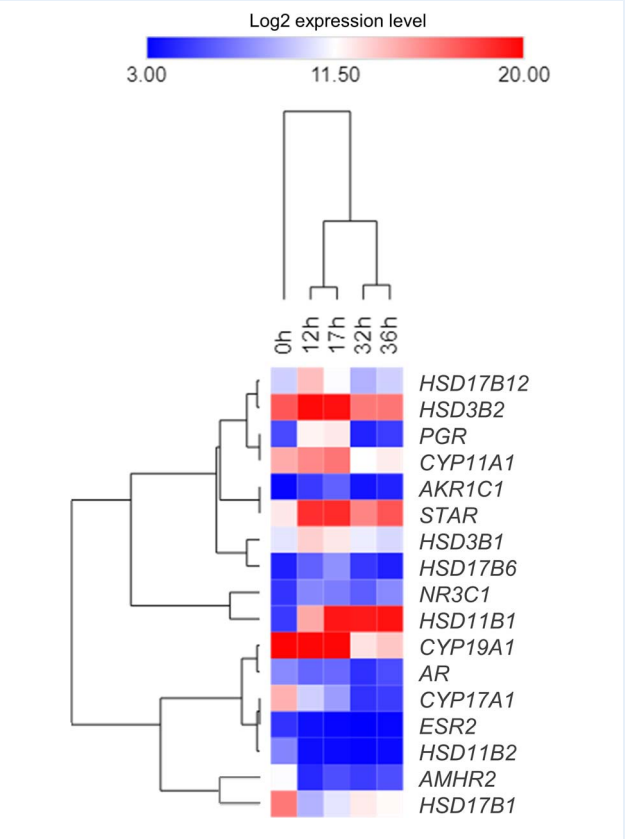

Figure 5 Heatmap and dendrogram of differentially expressed genes. Mean gene expression level (log2 transformed) across five time points before and up to 36 h after ovulation induction (OI), assessed by microarray analysis. The heat map only presents genes that changed significantly (FDR < 0.0001). Three overall clusters (top-down) represent genes that peaked midovulatory, genes that peaked at 36 h and genes that decreased after OI, respectively.

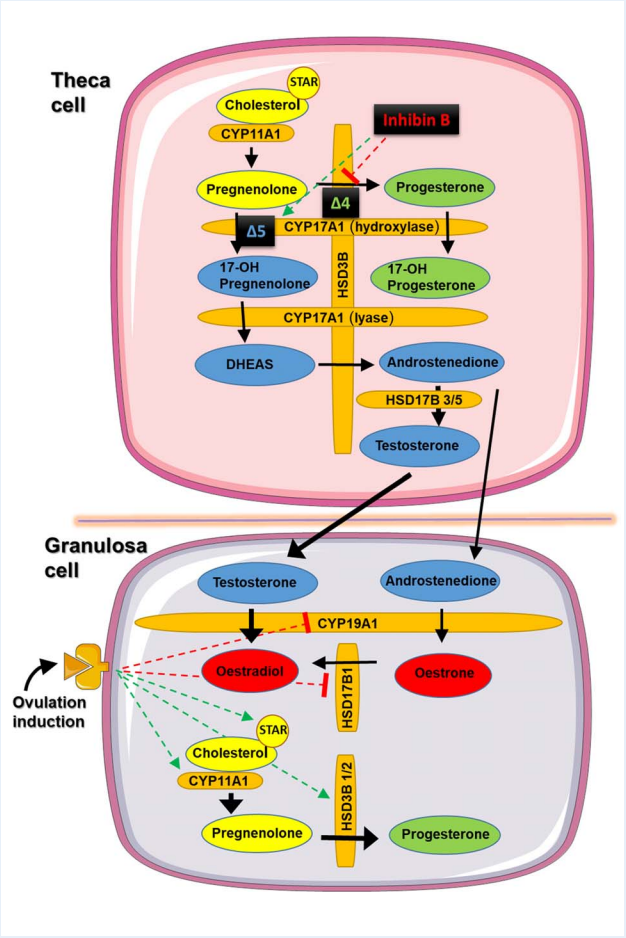

Figure 6 Proposed human ovarian steroidogenesis during ovulation. In theca cells, pregnenolone can be metabolized through the delta 4 or the delta 5-pathway, possibly regulated by inhibin B in favour of the delta 5-pathway. Androstenedione produced in the delta 5-pathway is converted to testosterone and both diffuse across the basal membrane into granulosa cells, where they are aromatized into oestradiol and oestrone, respectively. This pathway is downregulated after induction of ovulation. Conversely, in granulosa cells, upregulation of *STAR, CYP11A1* and *HSD3B1/2* after induction of ovulation secures massive production of progesterone, which is not converted any further in granulosa cells. The colours of steroids in the figure indicate the common steroid synthesis pathway (yellow), the delta 4-pathway for progesterone synthesis (green), the delta 5-pathway for androgen synthesis (blue) and the conversion of androgens intro oestrogens (red). Up or downregulation of steroidogenic enzymes in GCs after ovulation induction is indicated by dotted lines. Enlarged black arrows major routes in granulosa cells as suggested by the present study. Theca cells where not analysed in the present study, and the theca cell depiction is therefore based on previous studies and assumptions.

AMH concentrations measured in the present study (2–7 ng/mL) were quite similar to serum concentrations, but considerably lower than those previously observed in small antral follicles (800 ng/mL) (Andersen and Byskov, 2006). Circulating levels therefore do not reflect the ovulatory AMH production, but rather the production in preantral and small antral follicles (Weenen *et al.*, 2004; Jeppesen *et al.*, 2013). In antral follicles, AMH is involved in inhibition of FSH-induced CYP19A1 action (Dewailly *et al.*, 2016), and there is a well-established negative correlation between AMH and oestradiol concentration in the follicular phase (Andersen and Byskov, 2006; Dewailly *et al.*, 2016). The present study did not find a negative correlation between AMH and oestradiol, which may indicate that at the ovulary stage, oestradiol production is no longer influenced by the AMH concentrations present. Furthermore, the shutdown of *AMHR2* gene expression following OI strongly suggests that the intra-follicular roles of AMH after OI are negligible.

The present study showed that the ovulatory hormone dynamics as measured in one follicle from a cohort of approximately 12 mature follicles in women undergoing ovarian stimulation, paralleled the changes in circulating concentrations of oestradiol, inhibin A and inhibin B, which could therefore be used to monitor the intra-follicular changes. Furthermore, the GC progesterone production is reflected in circulation by both a progesterone increase and by a 17-hydroxyprogesterone increase and peak at 17 h. Interestingly, 17-hydroxyprogesterone presented low levels in FF, where it was not significantly altered, and this difference to plasma may be explained by the localization of CYP17A1 in TCs: a part of the FF progesterone may be converted into

17-hydroxyprogesterone as it crosses the TC layer moving towards the capillaries. Androstenedione was not significantly regulated in either FF or plasma, and the ratio between the compartments was only 1:2–1:3, which probably reflects that the majority of circulating androstenedione is produced in the adrenal glands (Burger, 2002).

This study of the physiological events of ovulation is limited by the application of ovarian stimulation, as differences to the natural cycle may exist. A previous study has found that FF steroid concentrations differ between natural and stimulated cycles at OPU (de los Santos *et al.*, 2012). In addition, the validation of the ELISAs showed that the concentrations measured by ELISA correlated linearly to the concentrations measured by mass spectrometry, but were generally overestimated, which has been shown before (Kushnir *et al.*, 2009). However, we believe that the study serves as a valid model to assess the dynamic change in FF and GCs, as well as the correlations between the measured FF hormones, which take place following the midcycle surge of gonadotropins, while the absolute hormone concentrations may be overestimated. The differential effects exerted by choice of treatment or trigger did not influence the significant regulation of measured hormones across the study time points.

Previous studies have measured FF hormone levels at OPU (Westergaard *et al.*, 2004; Andersen and Byskov, 2006; Andersen *et al.*, 2006; Smitz *et al.*, 2007; Humaidan *et al.*, 2011) and found considerable differences in the measured concentrations, probably exemplifying differences between treatment protocols, patients and methods of analysis. An earlier study measured steroid hormones in antral follicles at six stages of the natural menstrual cycle (McNatty, 1978), and some studies have measured FF hormones in antral follicles retrieved from women undergoing ovarian cryopreservation (Yding Andersen, 2017; Kristensen *et al.*, 2018). However, besides one study in IVF patients measuring FF hormone levels before OI and 36 h later (Wissing *et al.*, 2014), to our knowledge, no previous human studies have presented detailed analyses of ovulatory FF dynamics.

In conclusion, this study documents, for the first time in detail, the hormonal dynamics in the intra-follicular compartment during ovulation in women and shows that the changes are mostly reflected in circulation. Vast changes take place during the first 12–17 h after initiation of the ovulatory process. Activity of the responsible steroidogenic enzymes parallels the hormone concentrations: intra-follicular oestradiol decreases throughout ovulation and progesterone peaks approximately 17 h after OI. Major mid-ovulatory peaks of FF inhibins, progesterone and cortisol suggest important intra-follicular roles for oocyte maturation, follicle rupture and the hormonal priming of the reproductive organs, while decrease in FF testosterone, oestradiol and their designated receptors in GCs indicate their diminishing role. The results highlight the importance of comprehensive regulation of steroidogenesis during ovulation for reproductive success in humans.

Supplementary data

Supplementary data are available at *Molecular Human Reproduction* online.

Acknowledgements

The authors thank Marjo Westerdahl at the Laboratory of Reproductive Biology, Copenhagen, for performing the ELISA assays. Marcus Sjödin and Johan Lindberg from Swetox Bioanalysis unit are thanked for performing UPLC-MS steroid measurements. Statistical aid from the Section of Biostatistics, University of Copenhagen, Denmark, is greatly appreciated.

Authors' roles

L.C.P. designed and executed the cohort study, included patients and isolated GCs and FF, performed statistical analysis, interpreted results and drafted the manuscript. A.L.E.G. included patients and performed or supervised follicle punctures. A.S.A. and J.A.B. performed immunofluorescence microscopy and qRT-PCR analyses. L.S.M. collected materials for UPLC-validation experiments. P.D. performed the UPLC-validation experiments. O.Ø. performed and supervised the RNA isolation and microarray analysis and assisted with bioinformatic analyses. A.L.E.G., M.L.G. and C.Y.A. conceived the idea, designed the cohort study and interpreted the results. All authors critically revised the manuscript and approved the final version.

Funding

The study was funded by Interreg V Öresund-Kattegat-Skatterak through ReproUnion (www.reprounion.eu) and by a grant from the Region Zealand Research Foundation, Denmark.

Conflicts of interest

The authors have no conflicts of interest to disclose.

References

Aedo AR, Landgren BM, Diczfalusy E. Studies on ovarian and adrenal steroids at different phases of the menstrual cycle. 1. Dynamic changes during the periovulatory period. *Contraception* 1981;**23**: 107–124.

Affymetrix. *Microarray normalization using Signal Space Transformation with probe Guanine Cytosine Count Correction* [Internet]. 2019; Available from: https://tools.thermofisher.com/content/sfs/brochures/sst_gccn_whitepaper.pdf.

Alak BM, Smith GD, Woodruff TK, Stouffer RL, Wolf DP. Enhancement of primate oocyte maturation and fertilization in vitro by inhibin A and activin A. *Fertil Steril* 1996;**66**:646–653.

Andersen CY. Possible new mechanisms of cortisol action in female reproductive organs: physiological implications of the free hormone hypothesis. *J Endocrinol* 2002;**173**:211–217.

Andersen CY, Byskov AG. Estradiol and regulation of anti-Müllerian hormone, inhibin-A, and inhibin-B secretion: analysis of small antral and preovulatory human follicles' fluid. *J Clin Endocrinol Metab* 2006; **91**:4064–4069.

Andersen CY, Humaidan P, Ejdrup HB, Bungum L, Grøndahl ML, Westergaard LG. Hormonal characteristics of follicular fluid from women receiving either GnRH agonist or hCG for ovulation induction. *Hum Reprod* 2006;**21**:2126–2130.

Andersen CY, Schmidt KT, Kristensen SG, Rosendahl M, Byskov AG, Ernst E. Concentrations of AMH and inhibin-B in relation to follicular

diameter in normal human small antral follicles. *Hum Reprod* 2010; **25**:1282–1287.

Andersson S, Moghrabi N. Physiology and molecular genetics of 17 beta-hydroxysteroid dehydrogenases. *Steroids* 1997;**62**:143–147.

ASRM Practice Committee. The clinical relevance of luteal phase deficiency: a committee opinion. *Fertil Steril* 2012;**98**:1112–1117.

Belin F, Goudet G, Duchamp G, Gérard N. Intrafollicular concentrations of steroids and steroidogenic enzymes in relation to follicular development in the mare. *Biol Reprod* 2000;**62**:1335–1343.

Bishop CV, Hennebold JD, Kahl CA, Stouffer RL. Knockdown of progesterone receptor (PGR) in macaque granulosa cells disrupts ovulation and progesterone production1. *Biol Reprod* 2016;**94**:109.

Bolstad BM, Irizarry R, Astrand M, Speed TP. A comparison of normalization methods for high density oligonucleotide array data based on variance and bias. *Bioinformatics* 2003;**19**:185–193.

Burger HG. Androgen production in women. *Fertil Steril* 2002;**77**: S3–S5.

Chaffin CL, Hess DL, Stouffer RL. Dynamics of periovulatory steroidogenesis in the rhesus monkey follicle after ovarian stimulation. *Hum Reprod* 1999;**14**:642–649.

Choi Y, Wilson K, Hannon PR, Rosewell KL, Brännström M, Akin JW, Curry TE, Jo M. Coordinated regulation among progesterone, prostaglandins, and EGF-like factors in human ovulatory follicles. *J Clin Endocrinol Metab* 2017;**102**:1971–1982.

Conley AJ. Steroidogenesis in the preovulatory porcine follicle' United States Department of Agriculture, 4 Agricultural Research Service, Roman L. Hruska Meat Animal. *Biol Reprod* 1994;**661**:655–661.

Dafopoulos K, Mademtzis I, Vanakara P, Kallitsaris A, Stamatiou G, Kotsovassilis C, Messinis IE. Evidence that termination of the estradiol-induced luteinizing hormone surge in women is regulated by ovarian factors. *J Clin Endocrinol Metab* 2006;**91**:641–645 Narnia.

Dewailly D, Robin G, Peigne M, Decanter C, Pigny P, Catteau-Jonard S. Interactions between androgens, FSH, anti-Müllerian hormone and estradiol during folliculogenesis in the human normal and polycystic ovary. *Hum Reprod Update* 2016;**22**:709–724.

Fagerberg L, Hallström BM, Oksvold P, Kampf C, Djureinovic D, Odeberg J, Habuka M, Tahmasebpoor S, Danielsson A, Edlund K *et al.* Analysis of the human tissue-specific expression by genome-wide integration of transcriptomics and antibody-based proteomics. *Mol Cell Proteomics* 2014;**13**:397–406.

Fritz MA, McLachlan RI, Cohen NL, Dahl KD, Bremner WJ, Soules MR. Onset and characteristics of the midcycle surge in bioactive and immunoactive luteinizing hormone secretion in normal women: influence of physiological variations in periovulatory ovarian steroid hormone secretion. *J Clin Endocrinol Metab* 1992;**75**:489–493.

Ghersevich SA, Poutanen MH, Martikainen HK, Vihko RK. Expression of 17 beta-hydroxysteroid dehydrogenase in human granulosa cells: correlation with follicular size, cytochrome P450 aromatase activity and oestradiol production. *J Endocrinol* 1994;**143**:139–150.

Groome NP, Illingworth PJ, O'Brien M, Pai R, Rodger FE, Mather JP, McNeilly AS. Measurement of dimeric inhibin B throughout the human menstrual cycle. *J Clin Endocrinol Metab* 1996;**81**:1401–1405.

Hakkarainen J, Jokela H, Pakarinen P, Heikelä H, Kätkänaho L, Vandenput L, Ohlsson C, Zhang F-P, Poutanen M. Hydroxysteroid (17β)-dehydrogenase 1–deficient female mice present with normal puberty onset but are severely subfertile due to a defect in luteinization and progesterone production. *FASEB J* 2015;**29**:3806–3816.

Hao J, Tuck AR, Sjödin MOD, Lindberg J, Sand A, Niklasson B, Argyraki M, Hovatta O, Damdimopoulou P. Resveratrol supports and alpha-naphthoflavone disrupts growth of human ovarian follicles in an in vitro tissue culture model. *Toxicol Appl Pharmacol* 2018;**338**: 73–82.

Hibbert ML, Stouffer RL, Wolf DP, Zelinski-Wooten MB. Midcycle administration of a progesterone synthesis inhibitor prevents ovulation in primates. *Proc Natl Acad Sci* 1996;**93**:1897–1901.

Hillier SG, Whitelaw PF, Smyth CD. Follicular oestrogen synthesis: the "two-cell, two-gonadotrophin" model revisited. *Mol Cell Endocrinol* 1994;**100**:51–54.

Hoff J, Quigley N, Yen S. Hormonal dynamics in mid-cycle: a re-evaluation. *J Clin Endocrinol Metab* 1983;**57**:792–796.

Humaidan P, Westergaard LG, Mikkelsen AL, Fukuda M, Yding Andersen C. Levels of the epidermal growth factor-like peptide amphiregulin in follicular fluid reflect the mode of triggering ovulation: a comparison between gonadotrophin-releasing hormone agonist and urinary human chorionic gonadotrophin. *Fertil Steril* 2011;**95**:2034–2038 Elsevier Ltd.

Jeppesen JV, Anderson RA, Kelsey TW, Christiansen SL, Kristensen SG, Jayaprakasan K, Raine-Fenning N, Campbell BK, Yding Andersen C. Which follicles make the most anti-Mullerian hormone in humans? Evidence for an abrupt decline in AMH production at the time of follicle selection. *Mol Hum Reprod* 2013;**19**:519–527.

Katulski K, Bornstein S, Figiel M, Wand D, Warenik-Szymankiewicz A, Trzeciak WH. Typical hormonal profiles are accompanied by increased immunoreactivity of theca folliculi steroid 17 alpha-hydroxylase P450 in polycystic ovary syndrome. *J Endocrinol Invest* 1998;**21**:304–309.

Komar CM, Berndtson AK, Evans AC, Fortune JE. Decline in circulating estradiol during the periovulatory period is correlated with decreases in estradiol and androgen, and in messenger RNA for p450 aromatase and p450 17alpha-hydroxylase, in bovine preovulatory follicles. *Biol Reprod* 2001;**64**:1797–1805.

Kristensen SG, Andersen K, Clement CA, Franks S, Hardy K, Andersen CY. Expression of TGF-beta superfamily growth factors, their receptors, the associated SMADs and antagonists in five isolated size-matched populations of pre-antral follicles from normal human ovaries. *Mol Hum Reprod* 2014;**20**:293–308.

Kristensen SG, Mamsen LS, Jeppesen JV, Bøtkjær JA, Pors SE, Borgbo T, Ernst E, Macklon KT, Andersen CY. Hallmarks of human small antral follicle development: implications for regulation of ovarian steroidogenesis and selection of the dominant follicle. *Front Endocrinol (Lausanne)* 2018;**8**:376.

Kushnir MM, Naessen T, Kirilovas D, Chaika A, Nosenko J, Mogilevkina I, Rockwood AL, Carlstrom K, Bergquist J. Steroid profiles in ovarian follicular fluid from regularly menstruating women and women after ovarian stimulation. *Clin Chem* 2009;**55**:519–526.

Lee JR, Kim SH, Kim SM, Jee BC, Ku S-Y, Suh CS, Choi YM, Kim JG, Moon SY. Anti-Mullerian hormone dynamics during controlled ovarian hyperstimulation and optimal timing of measurement for outcome prediction. *Hum Reprod* 2010;**25**: 2597–2604.

Liu W, Xin Q, Wang X, Wang S, Wang H, Zhang W, Yang Y, Zhang Y, Zhang Z, Wang C *et al.* Estrogen receptors in granulosa cells govern meiotic resumption of pre-ovulatory oocytes in mammals. *Cell Death Dis* 2017;**8**:e2662.

Lockwood GM, Muttukrishna S, Groome NP, Knight PG, Ledger WL. Circulating inhibins and activin A during GnRH-analogue down-regulation and ovarian hyperstimulation with recombinant FSH for in-vitro fertilization-embryo transfer. *Clin Endocrinol (Oxf)* 1996; **45**:741–748.

de los Santos MJ, García-Láez V, Beltrán-Torregrosa D, Horcajadas JA, Martínez-Conejero JA, Esteban FJ, Pellicer A, Labarta E. Hormonal and molecular characterization of follicular fluid, cumulus cells and oocytes from pre-ovulatory follicles in stimulated and unstimulated cycles. *Hum Reprod* 2012;**27**:1596–1605.

McNatty KP. Cyclic changes in antral fluid hormone concentrations in humans. *Clin Endocrinol Metab* 1978;**7**:577–600.

Messinis IE, Messini CI, Dafopoulos K. Novel aspects of the endocrinology of the menstrual cycle. *Reprod Biomed Online* 2014;**28**:714–722.

Miller WL. Steroidogenic enzymes. *Endocr Dev* 2008;**13**:1–18 KARGER: Basel.

Nahum R, Thong KJ, Hillier SG. Metabolic regulation of androgen production by human thecal cells in vitro. *Hum Reprod* 1995;**10**:75–81.

Nelson VL, Qin KN, Rosenfield RL, Wood JR, Penning TM, Legro RS, Strauss JF, McAllister JM. The biochemical basis for increased testosterone production in theca cells propagated from patients with polycystic ovary syndrome. *J Clin Endocrinol Metab* 2001;**86**: 5925–5933.

Pelletier G, Li S, Luu-The V, Tremblay Y, Bélanger A, Labrie F. Immunoelectron microscopic localization of three key steroidogenic enzymes (cytochrome P450(scc), 3 beta-hydroxysteroid dehydrogenase and cytochrome P450(c17)) in rat adrenal cortex and gonads. *J Endocrinol* 2001;**171**:373–383.

Pelletier G, Luu-The V, Tětu B, Labrie F. Immunocytochemical localization of type 5 17 β-hydroxysteroid dehydrogenase in human reproductive tissues. *J Histochem Cytochem* 1999;**47**:731–737.

Poulsen L la C, Englund ALM, Wissing MLM, Yding Andersen C, Borup R, Grøndahl ML. Human granulosa cells function as innate immune cells executing an inflammatory reaction during ovulation: a microarray analysis. *Mol Cell Endocrinol* 2019a;**486**:34–46.

Poulsen L la C, Pla I, Sanchez A, Grøndahl ML, Marko-Varga G, Yding Andersen C, Englund ALM E, Malm J. Progressive changes in human follicular fluid composition over the course of ovulation: quantitative proteomic analyses. *Mol Cell Endocrinol* 2019b;**495**: 110522 Elsevier.

Robker RL, Russell DL, Espey LL, Lydon JP, O'Malley BW, Richards JS. Progesterone-regulated genes in the ovulation process: ADAMTS-1 and cathepsin L proteases. *Proc Natl Acad Sci* 2000;**97**:4689–4694.

Roos J, Johnson S, Weddell S, Godehardt E, Schiffner J, Freundl G, Gnoth C. Monitoring the menstrual cycle: comparison of urinary and serum reproductive hormones referenced to true ovulation. *Eur J Contracept Reprod Heal Care* 2015;**20**:438–450.

Schenken RS, Werlin LB, Williams RF, Prihoda TJ, Hodgen GD. Periovulatory hormonal dynamics: relationship of immunoassayable gonadotropins and ovarian steroids to the bioassayable luteinizing hormone surge in rhesus monkeys. *J Clin Endocrinol Metab* 1985; **60**:886–890.

Smitz J, Andersen AN, Devroey P, Arce J-C, MERIT Group. Endocrine profile in serum and follicular fluid differs after ovarian stimulation with HP-hMG or recombinant FSH in IVF patients. *Hum Reprod* 2007; **22**:676–687.

Smyth CD, Miró F, Whitelaw PF, Howles CM, Hillier SG. Ovarian thecal/interstitial androgen synthesis is enhanced by a follicle-stimulating hormone-stimulated paracrine mechanism. *Endocrinology* 1993;**133**:1532–1538.

Tamura T, Kitawaki J, Yamamoto T, Osawa Y, Kominami S, Takemori S, Okada H. Immunohistochemical localization of 17 alpha-hydroxylase/C17-20 lyase and aromatase cytochrome P-450 in the human ovary during the menstrual cycle. *J Endocrinol* 1992;**135**: 589–595.

Weenen C, Laven JSE, Bergh ARM Von, Cranfield M, Groome NP, Visser JA, Kramer P, Fauser BCJM, Themmen APN. Anti-Müllerian hormone expression pattern in the human ovary: potential implications for initial and cyclic follicle recruitment. *Mol Hum Reprod* 2004;**10**:77–83.

Westergaard LG, Erb K, Laursen SB, Rasmussen PE, Rex S, Westergaard CG, Andersen CY. Concentrations of gonadotrophins and steroids in pre-ovulatory follicular fluid and serum in relation to stimulation protocol and outcome of assisted reproduction treatment. *Reprod Biomed Online* 2004;**8**:516–523.

Whitelaw PF, Smyth CD, Howles CM, Hillier SG. Cell-specific expression of aromatase and LH receptor mRNAs in rat ovary. *J Mol Endocrinol* 1992;**9**:309–312.

Wissing ML, Kristensen SG, Andersen CY, Mikkelsen AL, Høst T, Borup R, Grøndahl ML. Identification of new ovulation-related genes in humans by comparing the transcriptome of granulosa cells before and after ovulation triggering in the same controlled ovarian stimulation cycle. *Hum Reprod* 2014;**29**:997–1010.

Yding Andersen C. Inhibin-B secretion and FSH isoform distribution may play an integral part of follicular selection in the natural menstrual cycle. *Mol Hum Reprod* 2017;**23**:16–24.